

# UC San Diego

## UC San Diego Previously Published Works

### Title

Probing sporadic and familial Alzheimer's disease using induced pluripotent stem cells.

### Permalink

<https://escholarship.org/uc/item/8q31t167>

### Journal

Nature, 482(7384)

### ISSN

0028-0836

### Authors

Israel, Mason A  
Yuan, Shauna H  
Bardy, Cedric  
[et al.](#)

### Publication Date

2012

### DOI

10.1038/nature10821

Peer reviewed



Published in final edited form as:

Nature. ; 482(7384): 216–220. doi:10.1038/nature10821.

## Probing sporadic and familial Alzheimer's disease using induced pluripotent stem cells

Mason A. Israel<sup>1,2</sup>, Shauna H. Yuan<sup>1,3</sup>, Cedric Bardy<sup>4</sup>, Sol M. Reyna<sup>1,2</sup>, Yangling Mu<sup>4</sup>, Cheryl Herrera<sup>1</sup>, Michael P. Hefferan<sup>5</sup>, Sebastiaan Van Gorp<sup>6</sup>, Kristopher L. Nazor<sup>7</sup>, Francesca S. Boscolo<sup>8</sup>, Christian T. Carson<sup>9</sup>, Louise C. Laurent<sup>8</sup>, Martin Marsala<sup>5,10</sup>, Fred H. Gage<sup>4</sup>, Anne M. Remes<sup>11</sup>, Edward H. Koo<sup>3</sup>, and Lawrence S. B. Goldstein<sup>1,3</sup>

<sup>1</sup>Howard Hughes Medical Institute and Department of Cellular and Molecular Medicine, University of California, San Diego, La Jolla, California 92093, USA <sup>2</sup>Biomedical Sciences Graduate Program, University of California, San Diego, La Jolla, California 92093, USA <sup>3</sup>Department of Neurosciences, University of California, San Diego, La Jolla, California, USA <sup>4</sup>The Salk Institute for Biological Studies, La Jolla, California 92037, USA <sup>5</sup>Department of Anesthesiology, University of California, San Diego, La Jolla, California 92093, USA <sup>6</sup>Department of Anesthesiology, Maastricht University Medical Center, Maastricht 6202 AZ, Netherlands <sup>7</sup>Department of Chemical Physiology, The Scripps Research Institute, La Jolla, California 92037, USA <sup>8</sup>Department of Reproductive Medicine, University of California, San Diego, La Jolla, California 92093, USA <sup>9</sup>BD Biosciences, La Jolla, California 92037, USA <sup>10</sup>Institute of Neurobiology, Slovak Academy of Sciences, Kosice SK-04001, Slovakia <sup>11</sup>Department of Clinical Medicine, Neurology and Clinical Research Center, University of Oulu, Oulu FIN-90015, Finland

### Abstract

Our understanding of Alzheimer's disease pathogenesis is currently limited by difficulties in obtaining live neurons from patients and the inability to model the sporadic form of the disease. It may be possible to overcome these challenges by reprogramming primary cells from patients into induced pluripotent stem cells (iPSCs). Here we reprogrammed primary fibroblasts from two patients with familial Alzheimer's disease, both caused by a duplication of the amyloid- $\beta$  precursor protein gene<sup>1</sup> (*APP*; termed APP<sup>DP</sup>), two with sporadic Alzheimer's disease (termed

Users may view, print, copy, download and text and data- mine the content in such documents, for the purposes of academic research, subject always to the full Conditions of use: [http://www.nature.com/authors/editorial\\_policies/license.html#terms](http://www.nature.com/authors/editorial_policies/license.html#terms)

Correspondence and requests for materials should be addressed to L.S.B.G. ([lgoldstein@ucsd.edu](mailto:lgoldstein@ucsd.edu)).

**Author Contributions** M.A.I. and L.S.B.G. conceived the project; M.A.I. and L.S.B.G. designed the experiments; M.A.I., S.H.Y., C.B., S.M.R., Y.M., C.H., M.P.H., S.V.G., M.M., K.L.N. and F.S.B. performed the experiments; M.A.I., S.H.Y. and C.T.C. developed differentiation methods; A.M.R. and E.H.K. provided APP<sup>DP</sup> patient samples and information; F.H.G. supervised C.B. and Y.M.; M.M. supervised M.P.H. and S.V.G.; L.C.L. supervised K.L.N. and F.S.B.; M.A.I. and L.S.B.G. wrote the manuscript; F.H.G., E.H.K. and A.M.R. edited the manuscript.

Data have been deposited in the Gene Expression Omnibus under accession GSE34879. Reprints and permissions information is available at [www.nature.com/reprints](http://www.nature.com/reprints).

The authors declare no competing financial interests.

Readers are welcome to comment on the online version of this article at [www.nature.com/nature](http://www.nature.com/nature).

Supplementary Information is linked to the online version of the paper at [www.nature.com/nature](http://www.nature.com/nature).

**Full Methods** and any associated references are available in the online version of the paper at [www.nature.com/nature](http://www.nature.com/nature).

sAD1, sAD2) and two non-demented control individuals into iPSC lines. Neurons from differentiated cultures were purified with fluorescence-activated cell sorting and characterized. Purified cultures contained more than 90% neurons, clustered with fetal brain messenger RNA samples by microarray criteria, and could form functional synaptic contacts. Virtually all cells exhibited normal electrophysiological activity. Relative to controls, iPSC-derived, purified neurons from the two APP<sup>Dp</sup> patients and patient sAD2 exhibited significantly higher levels of the pathological markers amyloid- $\beta$ (1–40), phospho-tau(Thr 231) and active glycogen synthase kinase-3 $\beta$  (aGSK-3 $\beta$ ). Neurons from APP<sup>Dp</sup> and sAD2 patients also accumulated large RAB5-positive early endosomes compared to controls. Treatment of purified neurons with  $\beta$ -secretase inhibitors, but not  $\gamma$ -secretase inhibitors, caused significant reductions in phospho-Tau(Thr 231) and aGSK-3 $\beta$  levels. These results suggest a direct relationship between APP proteolytic processing, but not amyloid- $\beta$ , in GSK-3 $\beta$  activation and tau phosphorylation in human neurons. Additionally, we observed that neurons with the genome of one sAD patient exhibited the phenotypes seen in familial Alzheimer's disease samples. More generally, we demonstrate that iPSC technology can be used to observe phenotypes relevant to Alzheimer's disease, even though it can take decades for overt disease to manifest in patients.

---

Alzheimer's disease is a common neurodegenerative disorder, defined post mortem by the increased presence of amyloid plaques and neurofibrillary tangles in the brain<sup>2</sup>. Amyloid plaques are extracellular deposits consisting primarily of amyloid- $\beta$  peptides, and neurofibrillary tangles are intraneuronal aggregations of hyperphosphorylated tau, a microtubule-associated protein involved in microtubule stabilization<sup>3</sup>. The causative relationship between amyloid plaque/amyloid- $\beta$  and tau pathologies is unclear in humans. Although the vast majority of Alzheimer's disease is apparently sporadic with significant non-Mendelian genetic contributions<sup>4</sup>, analyses of cellular and animal models of rare, dominantly inherited familial forms of Alzheimer's disease have driven most ideas about disease mechanisms. These rare cases have mutations or a duplication of *APP*, which encodes the amyloid- $\beta$  precursor protein, or mutations in the presenilin genes, which encode proteolytic enzymes that cleave APP into amyloid- $\beta$  and other fragments. Mouse models that overexpress familial Alzheimer's disease mutations develop extensive plaque deposition and amyloid-associated pathology, but neurofibrillary tangles and significant neuronal loss are conspicuously absent<sup>5,6</sup>. Fetal human cortical cultures have also been used to study the APP-tau relationship. For example, cortical cultures treated with 20  $\mu$ M amyloid- $\beta$  have elevated phosphorylated tau (p-tau)<sup>7</sup>. However, it is still unclear whether physiologically relevant levels of amyloid- $\beta$  directly cause elevated p-tau and which kinases are directly involved in this aberrant phosphorylation. Additionally, experimental approaches using fetal human neurons are hindered by limited availability of samples and unknown genetic backgrounds. The recent developments in iPSCs and induced neurons have allowed investigation of phenotypes of neurological diseases *in vitro*<sup>8,9,10</sup>. However, not all diseases have been successfully modelled using iPSCs<sup>11</sup>, and it is unclear whether iPSCs can be used to study sporadic forms of disease.

Here we report the derivation and neuronal differentiation of iPSCs from patients with familial and sporadic Alzheimer's disease, as well as from non-demented, age-matched controls. Using purified human neurons we probe three key questions concerning

Alzheimer's disease: (1) can iPSC technology be used to observe phenotypes of patients with Alzheimer's disease, even though it can take decades for overt disease to manifest; (2) is there a causative relationship between APP processing and tau phosphorylation; and (3) can neurons with the genome of a sAD patient exhibit phenotypes seen in familial Alzheimer's disease samples? Supplementary Fig. 1 summarizes the experimental approach and findings.

We characterized *APP* metabolism in fibroblasts before reprogramming to iPSCs (Supplementary Fig. 2). *APP* expression and amyloid- $\beta$  secretion were quantified in early-passage primary fibroblasts from two non-demented control (NDC) individuals, two sAD patients and two APP<sup>DP</sup> patients (Table 1). The presence of the genomic duplication was confirmed in fibroblasts. Relative to NDC and sAD cells, APP<sup>DP</sup> fibroblasts expressed higher levels of *APP* mRNA and secreted 1.5- to twofold higher amounts of amyloid- $\beta$ (1–40) peptides into culture media compared to NDC cells. We did not detect significant increases in amyloid- $\beta$ (1–42/1–40) or amyloid- $\beta$ (1–38/1–40) in patient samples versus controls.

We generated iPSC lines by transducing fibroblasts with retro-viruses encoding *OCT4*, *SOX2*, *KLF4*, *c-MYC* and, in one-third of cultures, *EGFP*. Each of the six individuals was represented by three clonal iPSC lines. All 18 iPSC lines maintained embryonic stem (ES)-cell-like morphology, expressed the pluripotency-associated proteins NANOG and TRA1-81, maintained euploid karyotypes, expressed endogenous locus-derived *SOX2*, repressed retroviral transgenes, and could differentiate into cells of ectodermal, mesodermal and endodermal lineages *in vitro* (Fig. 1a–d, Supplementary Figs 3a–e and 4). All lines tested (one per individual) formed teratomas when injected into nude rats (Supplementary Fig. 5). Supplementary Table 1 provides details of each iPSC line.

Variability in differentiation efficiency exists between pluripotent cell lines. To analyse variability in our iPSC lines, we used a fluorescence-activated cell sorting (FACS)-based method of neuronal differentiation and purification (summarized in Supplementary Fig. 6), based on work described previously<sup>12</sup>. Briefly, the 18 iPSC lines were first differentiated into cultures containing neural rosettes (Supplementary Fig. 3f). From these cultures, neural progenitor cells (NPCs) were purified and the efficiency of NPC formation was assessed by CD184<sup>+</sup>CD15<sup>+</sup>CD44<sup>-</sup>CD271<sup>-</sup> immunoreactivity. These FACS-purified NPCs maintained expression of NPC-associated markers, such as *SOX2* and nestin, over multiple passages (Fig. 1c, d). NPCs were differentiated for 3 weeks into heterogeneous cultures containing neurons (Supplementary Fig. 3g, h). *APP* copy number was faithfully maintained in differentiated cultures (Supplementary Fig. 3i). From these cultures, neurons were purified to near homogeneity, and the efficiency of neuron generation was assessed by CD24<sup>+</sup>CD184<sup>-</sup>CD44<sup>-</sup> immunoreactivity. No significant differences between any of the individuals in the efficiency of NPC or neuronal differentiation were detected (Fig. 1k, l).

Although we observed variability in differentiation among lines from each individual, the extent of inter-individual variation was less than observed intra-individual variability. These results suggest that any observed biochemical aberrations in neurons, if present in multiple lines derived from the same patient, are probably caused by features of that patient's

genotype. Purified neurons were plated at a density of  $2 \times 10^5$  cells per well of a 96-well plate and cultured for an additional 5 days. More than 90% of cells in these cultures were neurons, as judged by the presence of  $\beta$ III-tubulin<sup>+</sup>, MAP2<sup>+</sup> projections (Fig. 1e–h). Genome-wide mRNA expression profiles of five representative purified neuronal cultures were compared to the parental iPSC lines and samples from fetal brain, heart, liver and lung (Supplementary Fig. 7 and Supplementary Table 2). Unsupervised hierarchical clustering analysis revealed that purified neurons most closely resembled fetal brain samples, in part due to a global upregulation of neuronal genes. Interestingly, the largest difference between fetal brain samples and purified neurons was downregulation in purified neurons of the hippo signalling cascade (~6.1 fold), which regulates proliferation of cells such as NPCs and glia<sup>13,14</sup>.

We determined multiple electrophysiological properties of purified neurons to assess passive membrane properties and synaptic connectivity (Fig. 1i, j, Supplementary Table 3 and Supplementary Fig. 8). Notably, virtually all neurons tested generated voltage-dependent action potentials and currents (Fig. 1i), which were blocked by tetrodotoxin (Supplementary Fig. 8). Transient bath application of ionotropic receptor agonists (25  $\mu$ M muscimol or 10  $\mu$ M AMPA) evoked transient currents, showing that purified neurons expressed functional GABA and AMPA receptors, respectively (Supplementary Table 3). To determine whether neurons were also able to form functional synaptic contacts, we analysed continuous whole-cell voltage clamp recordings. We detected spontaneous inhibitory and/or excitatory synaptic currents in a subset of cells (~40%). Analysis of the kinetics of those events combined with reversible blockade using GABA<sub>A</sub> or AMPA receptor antagonists demonstrated that the neurons not only fire action potentials but also made functional synaptic contacts (Supplementary Table 3). The electrophysiological results were supported by analysis of expression of protein markers of glutamatergic and GABAergic neuronal subtypes (VGluT1 and GABA, respectively), which were detected by immunofluorescence, with approximately 15% of cells staining brightly for VGluT1 and 8% for GABA, and most remaining neurons staining dimly for one of the markers (Supplementary Fig. 9a). RNAs indicative of glutamatergic, GABAergic and cholinergic subtypes (that is, *VGLUT1*, *GAD67* and *CHAT*, respectively) were detected by quantitative polymerase chain reaction (qPCR). Importantly, no significant differences in neuronal subtypes were detected between patients and controls (Supplementary Fig. 9b–f).

Elevated or altered secretion of amyloid- $\beta$  peptides by fibroblasts is a feature common to all familial Alzheimer's disease mutations identified so far<sup>15,16</sup>. It is not known if iPSC-derived neurons from familial Alzheimer's disease patients maintain the elevated amyloid- $\beta$  production seen in the parental fibroblasts. In sAD fibroblasts and other peripheral cells, APP expression and amyloid- $\beta$  secretion are not consistently altered<sup>17</sup>. To determine if iPSC-derived neurons from APP<sup>DP</sup> and sAD patients exhibit elevated amyloid- $\beta$  secretion, amyloid- $\beta$  levels in neuron-conditioned media were measured and normalized to total protein levels of cell lysates. Purified neurons from patients APP<sup>DP1</sup> and APP<sup>DP2</sup>, each represented by three independently derived iPSC lines, secreted significantly higher levels of amyloid- $\beta$ (1–40) compared to mean NDC levels (Fig. 2a). Neurons from patient sAD2 also had significantly higher amyloid- $\beta$ (1–40) levels compared to NDC neurons, even

though no difference was observed between the fibroblasts of sAD2 and NDC individuals. We found that amyloid- $\beta$ (1–42) and amyloid- $\beta$ (1–38) levels in these purified neuronal cultures were often below the detection range of our assay, owing to the relatively small number of neurons purified. By cell type, neurons exhibited a larger difference in amyloid- $\beta$  levels between APP<sup>Dp</sup> and NDC than fibroblasts, further suggesting that fibroblasts are not fully predictive of neuronal phenotypes (Fig. 2b).

Genetic evidence implicates altered or elevated APP processing and amyloid- $\beta$  levels as the driving agents behind familial Alzheimer's disease<sup>2</sup> and, because of identical neuropathology, sporadic Alzheimer's disease. However, tau, although not genetically linked to Alzheimer's disease, forms neurofibrillary tangles, which correlate better with disease severity than plaque numbers<sup>18</sup>. The mechanism by which altered APP processing might cause elevated p-tau and neurofibrillary tangle pathology is unclear. Tau phosphorylation at Thr 231, one of several tau phosphoepitopes, regulates microtubule stability<sup>19</sup> and correlates with both neurofibrillary tangle number and degree of cognitive decline<sup>20,21</sup>. To determine if tau phosphorylation at Thr 231 is elevated in APP<sup>Dp</sup> and sAD neurons, we measured the amount of p-tau(Thr 231) relative to total tau levels in lysates from purified neurons from three iPSC lines from each of the NDC, sAD and APP<sup>Dp</sup> patients. Neurons from both APP<sup>Dp</sup> patients had significantly higher p-tau/total tau ratios than neurons from NDC lines (Fig. 2c). p-Tau/total tau in the two sAD patients mirrored the amyloid- $\beta$  findings: no difference was observed between sAD1 and NDC neurons whereas sAD2 neurons had significantly increased p-tau/total tau.

Tau can be phosphorylated by multiple kinases. The kinase GSK-3 $\beta$  can phosphorylate tau at Thr 231 *in vitro* and co-localizes with neurofibrillary tangles and pre-tangle phosphorylated tau in sAD postmortem neurons<sup>22</sup>. GSK-3 $\beta$  is thought to be constitutively active but is inactivated when phosphorylated at Ser 9 (ref. 23). To determine if iPSC-derived neurons with elevated p-tau have increased GSK-3 $\beta$  activity, the proportion of aGSK-3 $\beta$  in purified neurons was calculated by measuring the amount of GSK-3 $\beta$  lacking phosphorylation at Ser 9 relative to total GSK-3 $\beta$  levels. We observed that neurons from patients APP<sup>Dp</sup>1, APP<sup>Dp</sup>2 and sAD2 had significantly higher aGSK-3 $\beta$  than NDC neurons (Fig. 2d). The amyloid- $\beta$ , GSK-3 $\beta$  and tau findings of sAD2 were verified by analysing an additional two iPSC lines (sAD2.4 and sAD2.5; characterization in Supplementary Fig. 10), and we observed that levels remained consistently elevated (Fig. 2e). Results are detailed per patient in Supplementary Table 4a, per cell line in Supplementary Fig. 11, and per cell culture in Supplementary Table 5.

Although amyloid- $\beta$ , p-tau and GSK-3 $\beta$  clearly have roles in Alzheimer's disease pathogenesis, their relationship is unclear. We observed that iPSC-derived neurons exhibited strong or very strong correlations between amyloid- $\beta$ (1–40), p-tau/total tau and aGSK-3 $\beta$  levels (Fig. 2f and Supplementary Table 4b). We reasoned that if APP proteolytic products, such as amyloid- $\beta$  or carboxy-terminal fragments (CTFs), have a causative role in p-tau and aGSK-3 $\beta$  elevation, then inhibiting  $\gamma$ - or  $\beta$ -secretase activity could reduce p-tau and aGSK-3 $\beta$ . We treated purified neurons from NDC1, NDC2, sAD2 and APP<sup>Dp</sup>2 (2–3 iPSC lines each) with  $\gamma$ -secretase inhibitors (CPD-E and DAPT) or  $\beta$ -secretase inhibitors ( $\beta$ Si-II and OM99-2) for 24 h and measured amyloid- $\beta$ , GSK-3 $\beta$  and p-tau/total tau compared to



vehicle-treated samples. All inhibitors reduced amyloid- $\beta$ (1–40) by similar levels (32–45% in patient samples) (Fig. 2g). Intriguingly, for both sAD2 and APP<sup>Dp2</sup> neurons, we observed that  $\beta$ -secretase inhibitors significantly reduced aGSK-3 $\beta$  and p-tau/total tau (Fig. 2g, and shown per iPSC line in Supplementary Fig. 12). Neither  $\gamma$ -secretase inhibitor significantly differed from control-treated samples for aGSK-3 $\beta$  levels and p-tau/total tau.

We extended phenotypic characterization of sAD2 and APP<sup>Dp</sup> by analysing endosomal and synaptic markers in FACS-purified neurons co-cultured with astrocytes for 12 days. Accumulation of large RAB5<sup>+</sup> early endosomes in neurons has been observed in autopsies from sporadic Alzheimer's disease and some forms of familial Alzheimer's disease<sup>24,25</sup>. As  $\beta$ -secretase is localized to endosomes and has an acidic pH optimum, it has been proposed that early endosomes potentially mediate the effects of APP processing on downstream pathologies such as increased p-tau, neurofibrillary tangles, synaptic loss and apoptosis<sup>26</sup>; however, these hypotheses have been difficult to test directly without live, patient-specific neurons. To determine if early endosome phenotypes are present in iPSC-derived neurons from Alzheimer's disease patients, purified neurons from NDC1, NDC2, sAD2 and APP<sup>Dp2</sup> (two iPSC lines each) co-cultured with astrocytes were harvested and large and very large Rab5<sup>+</sup> early endosomes (1–2.1  $\mu\text{m}^3$  and 2.1–7  $\mu\text{m}^3$ ) in neuronal soma were counted. Whereas control neurons generally had few Rab5<sup>+</sup> structures  $>1 \mu\text{m}^3$ , neurons from both sAD2 and APP<sup>Dp2</sup> frequently had Rab5<sup>+</sup> early endosomes highly similar in volume, morphology and localization to what has been observed in autopsy samples (Fig. 3a–c). When compared, the neurons from both sAD2 and APP<sup>Dp2</sup> had significantly increased numbers of both large and very large early endosomes relative to controls (Fig. 3d). We sought to determine if neuronal cultures from sAD2 and APP<sup>Dp2</sup> also contained reduced levels of the presynaptic marker synapsin I. In Alzheimer's disease autopsies, synaptic loss is one of the strongest pathological correlates with dementia severity, and in regions of the brain affected by Alzheimer's disease, the presynaptic marker synapsin I is decreased in patients versus controls<sup>27,28</sup>. To analyse synapsin I levels in iPSC-derived neurons co-cultured with astrocytes, we quantified synapsin I<sup>+</sup> puncta on MAP2<sup>+</sup> dendrites (Fig. 3e). We found no significant difference between NDCs and either sAD2 or APP<sup>Dp2</sup> in the number of puncta per  $\mu\text{m}$  dendrite (Fig. 3f). Extended culture periods may be required to study Alzheimer's disease-associated loss of synaptic proteins.

The results of this study provide strong evidence that iPSC technology can be used in concert with post-mortem samples and animal models to study early pathogenesis and drug response in sporadic and familial Alzheimer's disease. In purified, electrophysiologically active neurons from one sporadic Alzheimer's disease and two APP<sup>Dp</sup> patients, each represented by at least three clonally derived iPSC lines, we observed significantly increased levels of three major biochemical markers of Alzheimer's disease: amyloid- $\beta$ (1–40), aGSK-3 $\beta$  and p-tau/total tau. Increased sAD2 amyloid- $\beta$  levels were not observed in the parental fibroblasts, suggesting a cell-type-specific phenotype. Among the individuals in this study, not only did strong correlations exist between amyloid- $\beta$ (1–40), p-tau/total tau and aGSK-3 $\beta$ , but both p-tau/total tau and aGSK-3 $\beta$  levels were also partially rescued in neurons from sAD2 and APP<sup>Dp</sup> following treatment with  $\beta$ -secretase inhibitors, suggesting that the APP processing pathway has a causative role in tau Thr 231 phosphorylation in human neurons. Because  $\gamma$ -secretase inhibition did not cause a significant effect, products of APP

processing other than amyloid- $\beta$  may have a role in induction of GSK-3 $\beta$  activity and p-tau. One potential culprit is the  $\beta$ -CTF, the levels of which correlate with axonopathies in mouse models harbouring APP duplications<sup>29</sup> and mediate early endosome accumulation in human Down's syndrome fibroblasts<sup>30</sup>. The observation that neurons from patients sAD2 and APP<sup>DP2</sup> have early endosome phenotypes raises the question of how aberrant early endosomes relate to other phenotypes of Alzheimer's disease, such as axonopathies, synaptic loss and cell death, in human neurons. Neurons and synapses rely heavily on endocytic pathways, and thus iPSC technology can now be used to study the role of this dynamic process in live patient-specific neurons. One point of caution is that it is possible that the cultures of purified neurons that we generated and studied may not have been fully mature, as they lacked repetitive action potentials and had limited spontaneous activity. Although some types of mature neurons also have these properties, it is conceivable that the phenotypes we observed might be modified by duration of *in vitro* culture. In this context, while there is debate about when Alzheimer's disease phenotypes initiate, evidence exists that Alzheimer's disease-like pathology can occur in Down's syndrome fetuses as early as 28 weeks of gestation<sup>24</sup>.

Our finding that the genome of patient sAD2, but not patient sAD1, generates significant Alzheimer's disease phenotypes in purified neurons has important implications. First, this finding suggests that an unknown frequency of sporadic Alzheimer's disease patients will have genomes that generate strong neuronal phenotypes. The frequency of such genomes in the sporadic Alzheimer's disease population cannot be determined from the small sample size we report and will require a larger sample size to ask how frequent such genomes are in the clinical population diagnosed with sporadic Alzheimer's disease. Second, the genome of sAD2 clearly harbours one or more variants that generate Alzheimer's disease phenotypes, which can thus be elucidated by future molecular genetic studies. Third, we speculate that sporadic Alzheimer's disease might be sub-divided depending on whether neurons themselves are altered, as in the case of sAD2, as opposed to other cell types such as astrocytes, which could be altered in other cases, for example, sAD1. Thus, future iPSC studies examining larger numbers of patients and controls have the potential to provide great insight into the mechanisms behind the observed heterogeneity in sporadic Alzheimer's disease pathogenesis, the role of different cell types, patient-specific drug responses, and prospective diagnostics.

## METHODS SUMMARY

### iPSC generation and differentiation

Primary fibroblast cultures were established from dermal punch biopsies taken from individuals following informed consent and Institutional Review Board approval. To generate iPSCs, fibroblasts were transduced with MMLV vectors containing the complementary DNAs for *OCT4*, *SOX2*, *KLF4*, *c-MYC* and  $\pm$  *EGFP*. iPSC-derived NPCs were differentiated for 3 weeks, neurons were purified by FACS, and amyloid- $\beta$ , p-tau/total tau and aGSK-3 $\beta$  were measured on purified control and mutant neurons from multiple lines cultured in parallel for an additional 5 days by multi-spot electrochemiluminescence assays (Meso Scale Diagnostics). Early endosomes were analysed by confocal microscopy on



purified neurons co-cultured with human astrocytes (Lonza) for 12 days. To ensure reproducible and consistent data, we found that it is important to differentiate and evaluate neurons from full sets of mutant and control iPSC lines together.

### Statistics

$P < 0.05$  was considered statistically significant. Individuals were statistically compared to the total NDC pool by Tukey's test. Drug responses were compared to controls by Dunnett's method.  $N$  values signify the total number of separate cultures analysed, with each iPSC line contributing equally to the total.

### Supplementary Material

Refer to Web version on PubMed Central for supplementary material.

### Acknowledgments

We thank D. Galasko, M. Sundsmo, J. Rivera, J. Fontaine, C. Gigliotti and B. Yu at the University of California, San Diego (UCSD) Alzheimer's Disease Research Center for patient samples and data (grant AGO 5131); S. Dowdy and N. Yoshioka for viral vectors; B. Balderas at BD Biosciences for antibodies; C. Santucci and S. Nguyen for teratoma assay assistance; the UCSD Neuroscience Microscopy Shared Facility (grant P30 NS047101); and Planned Parenthood of the Pacific Southwest for fetal brain specimens. Funding was from California Institute of Regenerative Medicine (CIRM) comprehensive grants (M.M., F.H.G., L.S.B.G.), CIRM predoctoral fellowship (M.A.I.), FP7 Marie Curie IOF (C.B.), Weatherstone Foundation fellowship (K.L.N.), National Institutes of Health K12 HD001259, the Hartwell Foundation (L.C.L., F.S.B.), the Lookout Fund and the McDonnell Foundation (F.H.G.). L.S.B.G. is an investigator with the Howard Hughes Medical Institute.

### References

1. Rovelet-Lecrux A, et al. APP locus duplication in a Finnish family with dementia and intracerebral haemorrhage. *J Neurol Neurosurg Psychiatry*. 2007; 78:1158–1159. [PubMed: 17442758]
2. Tanzi RE, Bertram L. Twenty years of the Alzheimer's disease amyloid hypothesis: a genetic perspective. *Cell*. 2005; 120:545–555. [PubMed: 15734686]
3. Ballatore C, Lee VMY, Trojanowski JQ. Tau-mediated neurodegeneration in Alzheimer's disease and related disorders. *Nature Rev Neurosci*. 2007; 8:663–672. [PubMed: 17684513]
4. Gatz M, et al. Role of genes and environments for explaining Alzheimer disease. *Arch Gen Psychiatry*. 2006; 63:168–174. [PubMed: 16461860]
5. Games D, et al. Alzheimer-type neuropathology in transgenic mice overexpressing V717F  $\beta$ -amyloid precursor protein. *Nature*. 1995; 373:523–527. [PubMed: 7845465]
6. Roberson ED, et al. Reducing endogenous tau ameliorates amyloid  $\beta$ -induced deficits in an Alzheimer's disease mouse model. *Science*. 2007; 316:750–754. [PubMed: 17478722]
7. Busciglio J, Lorenzo A, Yeh J, Yankner BA.  $\beta$ -Amyloid fibrils induce tau phosphorylation and loss of microtubule binding. *Neuron*. 1995; 14:879–888. [PubMed: 7718249]
8. Ebert AD, et al. Induced pluripotent stem cells from a spinal muscular atrophy patient. *Nature*. 2009; 457:277–280. [PubMed: 19098894]
9. Nguyen HN, et al. LRRK2 mutant iPSC-derived DA neurons demonstrate increased susceptibility to oxidative stress. *Cell Stem Cell*. 2011; 8:267–280. [PubMed: 21362567]
10. Qiang L, et al. Directed conversion of Alzheimer's disease patient skin fibroblasts into functional neurons. *Cell*. 2011; 3:359–371. [PubMed: 21816272]
11. Urbach A, Bar-Nur O, Daley GQ, Benvenisty N. Differential modeling of fragile X syndrome by human embryonic stem cells and induced pluripotent stem cells. *Cell Stem Cell*. 2010; 6:407–411. [PubMed: 20452313]

12. Yuan SH, et al. Cell-surface marker signatures for the isolation of neural stem cells, glia and neurons derived from human pluripotent stem cells. *PLoS ONE*. 2011; 6:e17540. [PubMed: 21407814]
13. Cao X, Pfaff SL, Gage FH. YAP regulates neural progenitor cell number via the TEA domain transcription factor. *Genes Dev*. 2008; 22:3320–3334. [PubMed: 19015275]
14. Reddy BV, Irvine KD. Regulation of *Drosophila* glial cell proliferation by Merlin-Hippo signaling. *Development*. 2011; 138:5201–5212. [PubMed: 22069188]
15. Citron M, et al. Excessive production of amyloid  $\beta$ -protein by peripheral cells of symptomatic and presymptomatic patients carrying the Swedish familial Alzheimer disease mutation. *Proc Natl Acad Sci USA*. 1994; 91:11993–11997. [PubMed: 7991571]
16. Scheuner D, et al. Secreted amyloid  $\beta$ -protein similar to that in the senile plaques of Alzheimer's disease is increased *in vivo* by the presenilin 1 and 2 and APP mutations linked to familial Alzheimer's disease. *Nature Med*. 1996; 2:864–870. [PubMed: 8705854]
17. Gasparini L, et al. Peripheral markers in testing pathophysiological hypotheses and diagnosing Alzheimer's disease. *FASEB J*. 1998; 12:17–34. [PubMed: 9438407]
18. Arriagada PV, Growdon JH, Hedley-Whyte ET, Hyman BT. Neurofibrillary tangles but not senile plaques parallel duration and severity of Alzheimer's disease. *Neurology*. 1992; 42:631. [PubMed: 1549228]
19. Cho JH, Johnson GVW. Primed phosphorylation of tau at Thr 231 by glycogen synthase kinase 3 $\beta$  (GSK3 $\beta$ ) plays a critical role in regulating tau's ability to bind and stabilize microtubules. *J Neurochem*. 2004; 88:349–358. [PubMed: 14690523]
20. Buerger K, et al. CSF tau protein phosphorylated at threonine 231 correlates with cognitive decline in MCI subjects. *Neurology*. 2002; 59:627–629. [PubMed: 12196665]
21. Buerger K, et al. CSF phosphorylated tau protein correlates with neocortical neurofibrillary pathology in Alzheimer's disease. *Brain*. 2006; 129:3035–3041. [PubMed: 17012293]
22. Cho J, Johnson G. Glycogen synthase kinase 3 $\beta$  phosphorylates tau at both primed and unprimed sites. *J Biol Chem*. 2003; 278:187–193. [PubMed: 12409305]
23. Dajani R, et al. Crystal structure of glycogen synthase kinase 3 $\beta$ : structural basis for phosphate-primed substrate specificity and autoinhibition. *Cell*. 2001; 105:721–732. [PubMed: 11440715]
24. Cataldo AM, et al. Endocytic pathway abnormalities precede amyloid  $\beta$  deposition in sporadic Alzheimer's disease and Down syndrome: differential effects of APOE genotype and presenilin mutations. *Am J Pathol*. 2000; 157:277–286. [PubMed: 10880397]
25. Cataldo A, et al. Endocytic disturbances distinguish among subtypes of Alzheimer's disease and related disorders. *Ann Neurol*. 2001; 50:661–665. [PubMed: 11706973]
26. Nixon RA. Endosome function and dysfunction in Alzheimer's disease and other neurodegenerative diseases. *Neurobiol Aging*. 2005; 26:373–382. [PubMed: 15639316]
27. Hamos JE, DeGennaro LJ, Drachman DA. Synaptic loss in Alzheimer's disease and other dementias. *Neurology*. 1989; 39:355–361. [PubMed: 2927643]
28. Qin S, Hu XY, Xu H, Zhou JN. Regional alteration of synapsin I in the hippocampal formation of Alzheimer's disease patients. *Acta Neuropathol*. 2004; 107:209–215. [PubMed: 14673601]
29. Salehi A, et al. Increased *App* expression in a mouse model of Down's syndrome disrupts NGF transport and causes cholinergic neuron degeneration. *Neuron*. 2006; 51:29–42. [PubMed: 16815330]
30. Jiang Y, et al. Alzheimer's-related endosome dysfunction in Down syndrome is A $\beta$ -independent but requires APP and is reversed by BACE-1 inhibition. *Proc Natl Acad Sci USA*. 2010; 107:1630–1635. [PubMed: 20080541]

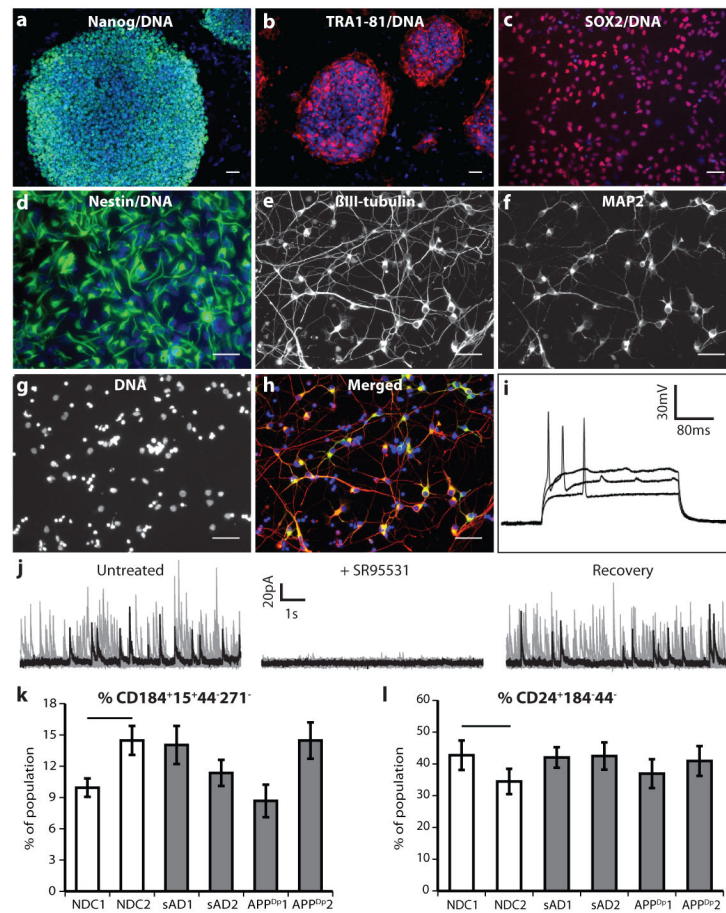


**Figure 1. Generation of iPSC lines and purified neurons from APP<sup>Dp</sup>, sAD and NDC fibroblasts**  
**a, b**, iPSC lines express NANOG and TRA1-81. **c, d**, iPSC-derived, FACS-purified NPCs express SOX2 and nestin. **e–h**, iPSC-derived, FACS-purified neurons express MAP2 and  $\beta$ III-tubulin. Scale bars in **a–h**, 50  $\mu$ m. **i**, Representative action potentials in response to somatic current injections. Data from iPSC line APP<sup>Dp</sup>2.2. **j**, Spontaneous synaptic activity was detected (voltage clamp recording at the reversal potential of sodium (0 mV)) and reversibly blocked by GABA<sub>A</sub> receptor antagonist SR95531 (10  $\mu$ M). Each panel represents ~4 min continuous recordings separated in 25 sweeps (grey traces) and superimposed for clarity. Black traces represent a single sweep. Data from iPSC line NDC2.1. **k, l**, No significant difference was seen between NDCs and any patient's cultures in the ability of iPSCs to generate NPCs at day 11 ( $P = 0.08$ ,  $n = 9$ ), or the ability of NPCs to form neurons at 3 weeks ( $P = 0.82$ ,  $n = 9$ ). Error bars indicate s.e.m.

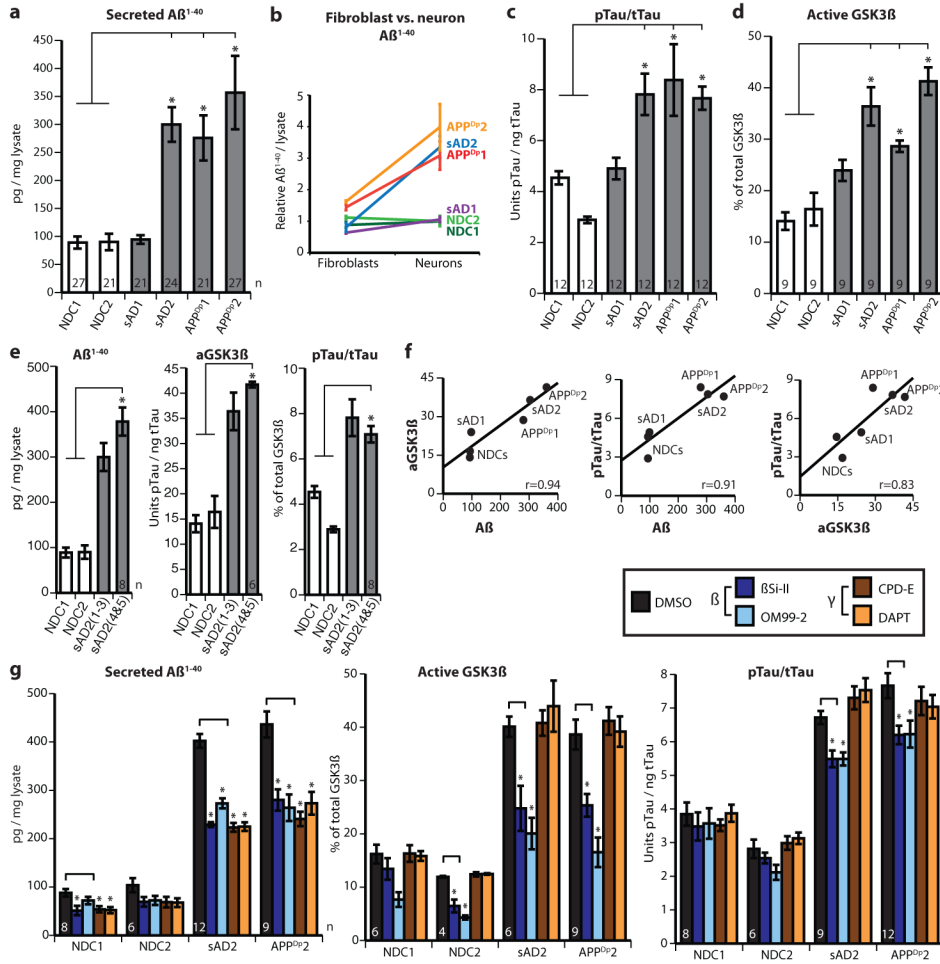


**Figure 2. Increased amyloid- $\beta$ , p-tau and aGSK-3 $\beta$  in sAD2 and APP<sup>DP</sup> neuronal cultures**  
**a**, Purified neurons from sAD2, APP<sup>DP</sup>P1 and APP<sup>DP</sup>P2 secrete increased amyloid- $\beta$ (1–40) (A $\beta$ (1–40)) compared to NDC samples ( $P = 0.0012, 0.0014$  and  $< 0.0001$ , respectively). **b**, Amyloid- $\beta$  differences between patients and controls are larger in neurons versus fibroblasts. Data sets are relative to NDC mean. **c, d**, Neurons from sAD2, APP<sup>DP</sup>P1 and APP<sup>DP</sup>P2 have increased aGSK-3 $\beta$  (percentage non-phospho-Ser 9) and p-tau/total tau (p-tau/t-tau) compared to NDC samples (aGSK-3 $\beta$ ,  $P < 0.0001, 0.0005$  and  $0.0001$ ; p-tau/total tau,  $P < 0.0001, 0.0001$  and  $0.0002$ ). In **a–d**,  $n$  values on graphs indicate the number of biological replicates per patient, contributed equally by three iPSC lines. **e**, sAD2 findings verified in two additional iPSC lines (sAD2.4 and sAD2.5). sAD2(1-3) indicates findings from initial sAD2 iPSC lines. For amyloid- $\beta$ , aGSK-3 $\beta$  and p-tau/total tau, sAD2 remained significantly higher than controls ( $P < 0.0001$ ). No significant difference was found between original and secondary sAD2 lines ( $P = 0.14, 0.44, 0.63$ ). **f**, Strong positive correlations between amyloid- $\beta$ (1–40), aGSK-3 $\beta$  and p-tau/total tau in purified neurons. Pearson  $R = 0.94, 0.91$  and  $0.83$ , respectively. **g**, Twenty-four hour treatment with  $\beta$ - and  $\gamma$ -secretase inhibitors reduced secreted amyloid- $\beta$ (1–40) compared to control treatment.  $\beta$ -Secretase inhibitors partially rescued aGSK-3 $\beta$  and p-tau/total tau in sAD2 and APP<sup>DP</sup>P2 neurons ( $P < 0.01$  for aGSK-3 $\beta$ ,  $P < 0.03$  for p-tau).  $\gamma$ -Secretase inhibition did not significantly affect aGSK-3 $\beta$

and p-tau/total tau. In **g**, number of treatment sets is indicated on the graph ( $n$ ), NDCs are represented by two iPSC lines each and sAD2 and APP<sup>Dp2</sup> are represented by three. Error bars indicate s.e.m.

Author Manuscript

Author Manuscript

Author Manuscript

Author Manuscript

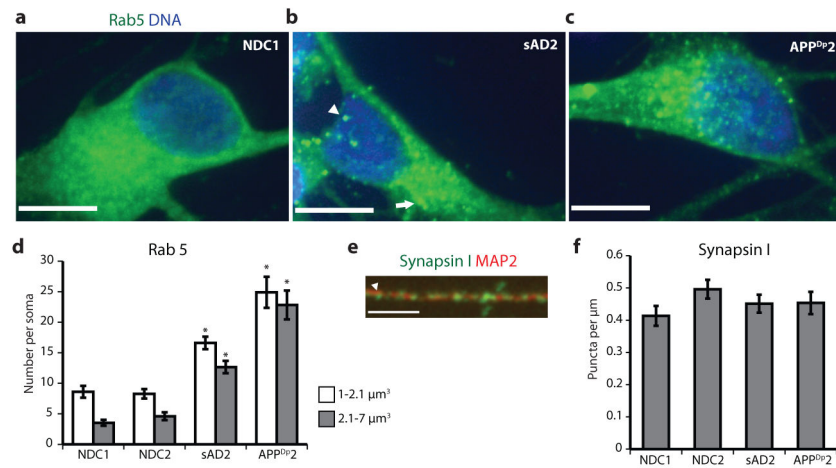


**Figure 3. Analysis of early endosome and synapsin levels in purified neurons co-cultured with astrocytes**

**a–c**, Extended focus images of Rab5-stained neuronal soma from NDC1, sAD2 and APP<sup>Dp2</sup>. Arrowhead in **b** marks a 1–2.1  $\mu\text{m}^3$  early endosome, and the arrow marks a 2.1–7  $\mu\text{m}^3$  early endosome. Scale bars, 10  $\mu\text{m}$ . **d**, Neurons from sAD2 and APP<sup>Dp2</sup> have significantly increased numbers of large and very large early endosomes compared to NDC neurons ( $P < 0.0001$ ,  $n = 40$  neurons from two iPSC lines per individual). **e**, Representative image of synapsin I (green) on a MAP2<sup>+</sup> dendrite (red). Arrowhead marks a synapsin I<sup>+</sup> punctum. Scale bar, 3  $\mu\text{m}$ . **f**, No significant difference between patients and controls in the number of synapsin<sup>+</sup> structures per  $\mu\text{m}$  dendrite ( $P = 1.00$ ,  $n = 40$  dendrites from two iPSC lines per individual). Neurons were scored blinded to genotype. Error bars indicate s.e.m.



**Table 1**

## Summary of patient information

Code	Diagnosis	Gender	Family history	Age at onset	Age at biopsy	MMSE at biopsy	APOE
NDC1	Non-demented control	M	Possible	N/A	86	30	2-3
NDC2	Non-demented control	M	N	N/A	86	30	3-3
sAD1	Sporadic AD	F	N	78	83	4	3-3
sAD2	Sporadic AD	M	N	78	83	18	3-3
APP <sup>DP1</sup>	Familial AD, APP duplication	M	Y	46	51	21	3-3
APP <sup>DP2</sup>	Familial AD, APP duplication	F	Y	53	60	17	3-3

MMSE, mini mental state examination (perfect score = 30). AD, Alzheimer's disease.